

MINERAL PARAGENESES OF BASIC TO INTERMEDIATE METAMORPHIC ROCKS IN THE YAMATO MOUNTAINS, EAST ANTARCTICA

Masao ASAMI

*Department of Geological Sciences, College of Liberal Arts, Okayama University,
1-1, Tsushima Naka 2-chome, Okayama 700*

and

Kazuyuki SHIRAISHI

National Institute of Polar Research, 9-10, Kaga 1-chome, Itabashi-ku, Tokyo 173

Abstract: Two groups of metamorphic rocks are found in association with syenitic and granitic rocks in the Yamato Mountains; Group I includes two-pyroxene-bearing gneiss and amphibolite, whereas Group II consists of granitic gneiss and associated rocks accompanied by no orthopyroxene. Mineral parageneses of basic to intermediate metamorphic rocks of the two groups were examined in the simplified system $\text{Al}_2\text{O}_3\text{-FeO-MgO-CaO-Na}_2\text{O}$.

Microprobe analyses reveal that hornblende of Group I is of pargasitic composition but hornblende of Group II has broad compositions ranging from tremolitic to pargasitic ones. Mineral parageneses of the two groups are incompatible with each other in such ways that the hornblende-plagioclase assemblage of Group I has higher $(\text{Na}/\text{Ca})_{\text{Hb}}^{\text{M}4}/(\text{Na}/\text{Ca})_{\text{Pl}}$ values than that of Group II, and that the clinopyroxene-hornblende tie lines of Group II are mostly included in the two-pyroxene-hornblende triangles of Group I in the $\text{Al}_2\text{O}_3\text{-FeO-MgO-CaO}$ tetrahedron. The hornblende-bearing assemblages of Group II are considered to be of the amphibolite facies but not the granulite facies.

Although no direct contact between the granulite-facies and amphibolite-facies metamorphic rocks has been found in the Yamato Mountains, the geological and petrological relations of the syenitic rocks to the metamorphic rocks suggest that the granulite-facies rocks and the syenitic rocks form a geological unit which is in tectonic contact with the other geological unit composed of the amphibolite-facies rocks.

1. Introduction

The Yamato Mountains, situated around lat. $71^{\circ}30'S$ and long. $35^{\circ}45'E$, are underlain by high-grade metamorphic rocks of various compositions and plutonic rocks of syenitic and granitic compositions. Geology and petrography of these basement rocks have been reported by KIZAKI (1965), OHTA and KIZAKI (1966), YOSHIDA and ANDO (1971), SHIRAISHI (1977), SHIRAISHI *et al.* (1978, 1982a, b, 1983) and YANAI *et al.* (1982). Metamorphic rocks of basic to intermediate compositions occur ubiquitously in this region. Among them, two-pyroxene-bearing mineral assemblages and orthopyroxene-free ones have been studied from petrogenetic points of view. KIZAKI (1965) and SHIRAISHI (1977) explained the latter assemblages to be those of the amphibolite

facies which resulted from granitization of the former granulite-facies ones. However, if the bulk compositions of rocks are inappropriate for the formation of orthopyroxene, some kinds of hornblende may be still stable even under the granulite-facies conditions.

We examined the mineral parageneses of basic to intermediate metamorphic rocks in order to clarify the factors controlling paragenetic relations between orthopyroxene-bearing mineral assemblages and orthopyroxene-free ones.

2. Geological and Petrographical Outlines

The Yamato Mountains consist of seven Massifs, A, B, C, D, E, F and G, which range for 50 km from south to north. There occur high-grade regional metamorphic rocks, syenitic rocks and granitic rocks. Figure 1 shows the compiled geological map of this region.

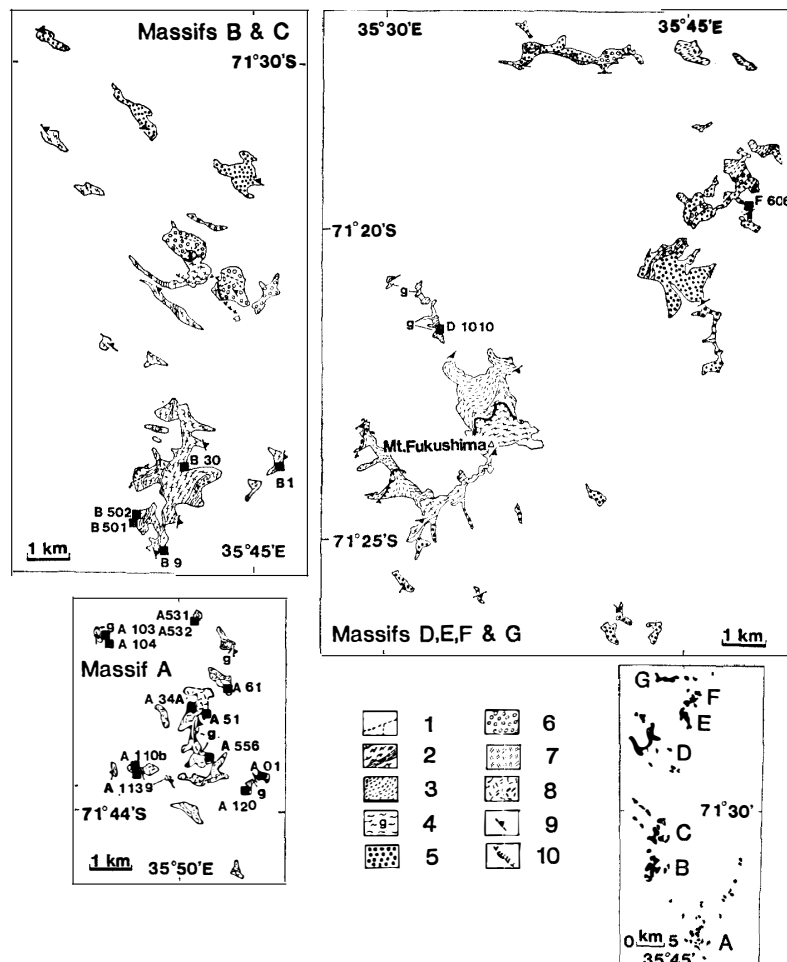


Fig. 1. Geological map of the Yamato Mountains. Localities of the specimens examined are shown. 1: Granite and pegmatite, 2: Granitic gneiss and biotite amphibolite, 3: Migmatitic gneiss, 4: Two-pyroxene-biotite gneiss and associated rocks, 5: Clinopyroxene syenite, 6: Porphyritic two-pyroxene syenite, 7: Clinopyroxene quartz monzo-syenite, 8: Two-pyroxene syenite, 9: Foliation, 10: Thrust fault.

Table 1. Rock types and mineral assemblages of metamorphic rocks.

Group I*	Group II**
(1) Two-pyroxene-biotite gneiss and associated rocks (Two-pyroxene-biotite gneiss) Op+Cp+Bi+Kf+Pl+Qz (\pm Hb) Op+Cp+Bi+Pl+Qz (\pm Hb) (Orthopyroxene-biotite gneiss) Op+Bi+Pl+Qz (\pm Kf) Op+Sp+Bi+Pl (Two-pyroxene amphibolite) Op+Cp+Hb+Bi+Pl (\pm Qz) (Clinopyroxene-hornblende-biotite gneiss) Cp+Hb+Bi+Pl+Qz (\pm Kf) (Calc-silicate gneiss) Gt+Wo+Cp+Sc+Qz+Sph (\pm Pl) Wo+Cp+Sc+Pl+Sph Wo+Cp+Sc+Cc+Sph Cp+Sc+Qz+Sph (\pm Hb)	(3) Granitic gneiss and associated rocks (Granitic gneiss) Bi+Kf+Pl+Qz Hb+Bi+Kf+Pl+Qz Cp+Hb+Bi+Kf+Pl+Qz (Biotite amphibolite) Hb+Bi+Kf+Pl+Qz Cp+Hb+Bi+Kf+Pl+Qz (Clinopyroxene-biotite gneiss) Cp+Bi+Kf+Pl+Qz (\pm Hb)
(2) Paleosome of migmatitic gneiss (Two-pyroxene-biotite gneiss) Op+Cp+Hb+Bi+Kf+Pl+Qz (Two-pyroxene amphibolite) Op+Cp+Hb+Bi+Pl (Clinopyroxene-biotite-K-feldspar rock) Cp+Bi+Kf+Pl+Qz	Abbreviations: Al-allanite, Ap-apatite, Bi-biotite, Cc-calcite, Cp-clinopyroxene, Gt-garnet, Hb-hornblende, Il-ilmenite, Kf-K-feldspar, Mt-magnetite, Op-orthopyroxene, Pl-plagioclase, Prh-pyrrhotite, Py-pyrite, Qz-quartz, Sc-scapolite, Sp-spinel, Sph-sphene, Wo-wollastonite, Zr-zircon

* +Il+Ap+Zr(\pm Mt, \pm Prh, \pm py), except for calc-silicate gneiss

** +Mt+Sph+Ap+Zr(\pm Il, \pm Py, \pm Al)

Metamorphic rocks are found in all the massifs. They are acid to basic, pelitic, psammitic and calcareous in composition, but basic to intermediate rocks are ubiquitous in occurrence. The metamorphic rocks can be classified into three groups on the basis of the field occurrence and petrographical characters: (1) two-pyroxene-biotite gneiss and associated rocks in Massifs A, D and G, (2) migmatitic gneiss in Massifs D, E, F and G, and (3) granitic gneiss and associated rocks in Massifs B, C and D (Fig. 1). Table 1 presents rock types and their mineral assemblages of the three groups. The rocks of the left category in Table 1 (Group I) are characterized by two-pyroxene-bearing assemblages, whereas those of the right (Group II) are orthopyroxene-free ones.

Further geological and petrographical descriptions of the metamorphic rocks in this region are given in SHIRAISHI *et al.* (1982a, b).

3. Method

Nine rock specimens from Group I and five specimens from Group II were selected for microprobe analyses of minerals. Rock types and mineral assemblages of these metamorphic rocks are listed in Table 2, and their localities are shown in Fig. 1. Eleven of the fourteen specimens contain hornblende. No textural evidence suggesting disequilibrium can be observed in the selected specimens.

Table 2. Rock types and mineral assemblages of specimens examined.

Rock types	Op	Cp	Hb	Bi	Pl(An%)	Kf	Qz	Il	Mt	Prh	Py	Sph	Others
Group I													
Y80A61	2Px-Bi gneiss	+	+		+	29-30	+	+			+		Ap,Zr
Y80A113	2Px-Bi gneiss	+	+		+	23-26	+	+	+				Ap,Zr
Y80A104	2Px-Bi gneiss	+	+	+	+	34-38		+	+				Ap,Zr
D73121010	2px-Bi gneiss	+	+	+	+	22-25	+	+	+			+	Ap,Zr
Y80A110b	2Px amphibolite	+	+	+	+	52-67		+	+			+	Ap,Zr
Y80A120	2Px amphibolite	+	+	+	+	53-68		+	+			+	Ap
Y80A531	2Px amphibolite	+	+	+	+	33-41			+		+		Ap
Y80A532	Cp-Hb-Bi gneiss		+	+	+	27-30		+	+		+	+	Ap
Y80A103	Cp-Hb-Bi gneiss		+	+	+	28-29	+	+					Al,Ap,Zr
Group II													
Y80B1	Granitic gneiss		+	+	+	25-27	+	+		+	+	+	Al,Ap,Zr
Y80B30	Granitic gneiss		+	+	+	4-9	+	+		+	+	+	Ap
Y80B9	Cp-Bi gneiss		+	+	+	19-21	+	+		+	+	+	Al,Ap,Zr
Y80B502	Bi amphibolite			+	+	26-34	+	+		+	+	+	Ap,Zr
Y80B501	Granitic gneiss				+	17-20	+	+	+	+	+	+	Zr

Abbreviations of mineral names refer to those in Table 1.

Table 3. Representative microprobe analyses of orthopyroxene.

	Y80A61	Y80A113	Y80A104	D73121010	Y80A110b	Y80A120	Y80A531
SiO ₂	49.83	50.56	50.63	49.88	50.89	51.92	49.06
TiO ₂	0.05	0.03	0.11	0.09	0.14	0.05	0.12
Al ₂ O ₃	0.32	0.29	0.27	0.56	0.49	0.49	0.39
Cr ₂ O ₃	0.00	0.00	0.02	0.00	0.11	0.04	0.10
FeO*	31.53	28.80	35.23	30.05	34.03	27.03	34.83
MnO	1.61	1.36	0.70	1.11	0.69	0.78	1.13
MgO	15.32	15.45	13.11	16.54	13.82	19.10	12.87
CaO	0.74	0.58	0.54	0.79	1.24	0.55	0.88
Na ₂ O	0.00	0.05	0.00	0.04	0.00	0.00	0.00
K ₂ O	0.00	0.05	0.03	0.00	0.02	0.03	0.00
NiO	0.06	0.00	0.03	0.00	0.00	0.00	0.04
Total	99.46	97.17	100.67	99.06	101.43	99.99	99.42
	6(O)						
Si	1.971	2.014	1.997	1.962	1.983	1.982	1.971
Al	0.015	0.014	0.012	0.026	0.022	0.022	0.018
Ti	0.002	0.001	0.003	0.003	0.004	0.001	0.004
Cr	—	—	0.001	—	0.003	0.001	0.003
Fe	1.043	0.959	1.162	0.989	1.109	0.863	1.170
Mn	0.054	0.046	0.023	0.037	0.023	0.025	0.038
Mg	0.903	0.917	0.771	0.970	0.803	1.087	0.771
Ca	0.031	0.025	0.023	0.033	0.052	0.022	0.038
Na	—	0.004	—	0.003	—	—	—
K	—	0.003	0.001	—	0.001	0.001	—
Ni	0.002	—	0.001	—	—	—	0.001
X _{Fe}	0.536	0.511	0.601	0.505	0.580	0.443	0.603

* Total iron as FeO. $X_{Fe} = Fe / (Fe + Mg)$.

Table 4. Representative microprobe analyses of clinopyroxene.

	Group I								Group II		
	Y80A61	Y80A113	Y80A104	D73121010	Y80A110b	Y80A120	Y80A531	Y80A532	Y80B1	Y80B30	Y80B9
SiO ₂	51.93	51.53	52.18	51.59	51.93	52.87	51.08	52.47	51.76	52.74	52.35
TiO ₂	0.06	0.15	0.11	0.11	0.09	0.17	0.15	0.15	0.11	0.15	0.09
Al ₂ O ₃	0.77	0.77	0.77	0.71	1.06	1.31	0.92	0.88	0.82	0.74	0.71
Cr ₂ O ₃	0.02	0.08	0.06	0.05	0.00	0.29	0.01	0.00	0.04	0.02	0.13
FeO*	12.80	12.32	14.36	11.18	14.00	9.05	15.15	12.14	10.89	8.22	8.91
MnO	0.57	0.48	0.40	0.37	0.21	0.43	0.51	0.60	0.89	0.51	0.57
MgO	11.79	11.65	10.17	12.41	10.82	13.75	10.20	11.22	12.31	13.35	13.42
CaO	21.68	21.36	21.26	21.79	22.05	22.63	21.43	22.71	23.20	22.47	23.66
Na ₂ O	0.38	0.31	0.27	0.50	0.30	0.29	0.33	0.38	0.40	0.88	0.51
K ₂ O	0.06	0.00	0.01	0.00	0.00	0.03	0.01	0.00	0.01	0.02	0.00
NiO	0.00	0.00	0.05	0.00	0.00	0.04	0.00	0.03	0.03	0.06	0.00
Total	100.06	98.65	99.64	98.71	100.46	100.86	99.79	100.58	100.46	99.16	100.34
	6(O)										
Si	1.975	1.982	2.000	1.976	1.975	1.962	1.970	1.982	1.957	1.987	1.963
Al	0.034	0.035	0.035	0.032	0.048	0.057	0.042	0.039	0.037	0.033	0.031
Ti	0.002	0.004	0.003	0.003	0.003	0.005	0.004	0.004	0.003	0.004	0.002
Cr	0.001	0.002	0.002	0.001	—	0.009	—	—	0.001	0.001	0.004
Fe	0.407	0.396	0.460	0.360	0.445	0.281	0.488	0.383	0.344	0.259	0.279
Mn	0.018	0.016	0.013	0.012	0.007	0.014	0.017	0.019	0.029	0.016	0.018
Mg	0.669	0.668	0.581	0.708	0.613	0.761	0.586	0.632	0.694	0.750	0.750
Ca	0.884	0.880	0.873	0.894	0.898	0.900	0.885	0.919	0.940	0.907	0.951
Na	0.028	0.023	0.020	0.037	0.022	0.021	0.025	0.027	0.029	0.064	0.037
K	0.003	—	0.001	—	—	0.001	—	—	0.001	0.001	—
Ni	—	—	0.001	—	—	0.001	—	0.001	0.001	0.002	—
X _{Fe}	0.378	0.372	0.442	0.337	0.421	0.270	0.454	0.377	0.331	0.257	0.271

* Total iron as FeO. $X_{Fe} = Fe / (Fe + Mg)$.

Table 5. Representative microprobe analyses of hornblende.

	Group I							Group II			
	Y80A104	D73121010	Y80A110b	Y80A120	Y80A531	Y80A532	Y80A103	Y80B1	Y80B30	Y80B9	Y80B502
SiO ₂	42.69	44.25	43.23	44.59	42.10	43.80	41.30	44.27	50.26	50.82	42.74
TiO ₂	1.64	1.44	1.92	1.89	2.06	1.72	0.66	1.01	0.60	0.46	1.69
Al ₂ O ₃	10.89	8.65	10.41	10.20	10.14	9.79	10.34	8.95	4.18	4.19	9.62
Cr ₂ O ₃	0.02	0.17	0.07	0.43	0.00	0.14	0.05	0.01	0.00	0.02	0.00
FeO*	20.21	15.44	18.33	12.79	20.77	17.59	22.32	18.15	11.03	12.42	18.81
MnO	0.23	0.29	0.08	0.26	0.29	0.37	0.54	0.44	0.29	0.36	0.29
MgO	7.83	11.23	9.32	13.12	7.96	9.48	6.97	9.89	16.48	16.09	9.73
CaO	10.99	11.18	11.43	11.51	11.48	11.34	10.99	11.80	12.07	11.73	11.71
Na ₂ O	1.21	1.85	1.60	1.75	1.71	1.46	1.22	1.41	1.35	0.95	1.63
K ₂ O	1.51	1.16	1.40	1.12	1.45	1.61	1.40	1.23	0.48	0.54	1.33
NiO	0.06	0.06	0.09	0.00	0.00	0.01	0.07	0.10	0.00	0.00	0.04
Total	97.28	95.72	97.88	97.66	97.96	97.31	95.86	97.26	96.74	97.58	97.59
23(O)											
Si	6.553	6.757	6.546	6.584	6.474	6.654	6.536	6.739	7.345	7.385	6.532
Al	1.971	1.557	1.858	1.774	1.837	1.753	1.928	1.606	0.720	0.718	1.732
Ti	0.189	0.166	0.218	0.210	0.238	0.197	0.078	0.116	0.066	0.051	0.195
Cr	0.003	0.020	0.009	0.050	—	0.016	0.006	0.001	—	0.002	—
Fe	2.594	1.972	2.322	1.579	2.671	2.234	2.954	2.311	1.348	1.509	2.403
Mn	0.029	0.038	0.010	0.032	0.037	0.048	0.073	0.056	0.036	0.044	0.038
Mg	1.791	2.557	2.105	2.888	1.824	2.146	1.645	2.245	3.589	3.486	2.216
Ca	1.807	1.830	1.854	1.821	1.891	1.846	1.863	1.925	1.889	1.826	1.917
Na	0.360	0.546	0.470	0.501	0.508	0.429	0.374	0.417	0.384	0.268	0.484
K	0.296	0.225	0.269	0.210	0.285	0.313	0.283	0.240	0.089	0.100	0.259
Ni	0.007	0.007	0.011	—	—	0.001	0.008	0.012	—	—	0.005
X _{Fe}	0.592	0.435	0.525	0.353	0.594	0.510	0.642	0.507	0.273	0.302	0.520

* Total iron as FeO. $X_{Fe} = Fe/(Fe + Mg)$.

Table 6. Representative microprobe analyses of biotite.

	Group I								Group II				
	Y80A61	Y80A113	Y80A104	D73121010	Y80A120	Y80A531	Y80A532	Y80A103	Y80B1	Y80B30	Y80B9	Y80B502	Y80A501
SiO ₂	36.76	36.61	35.35	37.96	37.80	35.88	36.49	35.63	37.49	37.93	38.86	36.60	36.48
TiO ₂	4.52	5.41	4.91	3.40	4.69	5.12	4.49	2.61	3.13	3.46	3.26	4.21	3.40
Al ₂ O ₃	13.86	12.55	13.48	12.72	13.42	13.60	12.98	14.08	14.07	12.77	12.97	13.34	13.37
Cr ₂ O ₃	0.10	0.00	0.04	0.14	0.45	0.00	0.14	0.01	0.05	0.03	0.24	0.01	0.00
FeO*	19.14	16.96	22.28	16.87	13.87	21.63	19.84	23.74	19.13	15.22	16.18	19.94	20.41
MnO	0.13	0.10	0.12	0.08	0.05	0.14	0.18	0.17	0.11	0.19	0.12	0.00	0.21
MgO	11.79	12.10	9.10	14.56	15.16	9.68	12.24	9.52	12.83	15.80	15.72	11.83	11.53
CaO	0.01	0.03	0.00	0.03	0.01	0.00	0.20	0.03	0.05	0.06	0.03	0.00	0.03
Na ₂ O	0.06	0.04	0.06	0.11	0.08	0.00	0.02	0.11	0.10	0.16	0.06	0.05	0.00
K ₂ O	8.58	8.69	8.43	9.29	9.59	9.58	8.90	7.93	9.47	9.33	9.37	8.89	9.10
NiO	0.00	0.04	0.00	0.04	0.07	0.05	0.00	0.04	0.08	0.00	0.06	0.07	0.00
Total	94.95	92.53	93.77	95.20	95.19	95.68	95.48	93.87	96.51	94.95	96.87	94.94	94.53
22(O)													
Si	5.609	5.693	5.569	5.732	5.641	5.548	5.585	5.619	5.646	5.705	5.736	5.624	5.654
Al	2.493	2.300	2.501	2.265	2.361	2.478	2.341	2.617	2.497	2.263	2.257	2.414	2.441
Ti	0.518	0.633	0.581	0.386	0.527	0.595	0.516	0.310	0.354	0.392	0.362	0.486	0.400
Cr	0.012	—	0.005	0.005	0.053	—	0.017	0.002	0.005	0.003	0.028	0.002	—
Fe	2.443	2.205	2.934	2.131	1.731	2.798	2.540	3.130	2.410	1.914	1.998	2.561	2.645
Mn	0.016	0.013	0.015	0.011	0.007	0.018	0.024	0.023	0.014	0.024	0.016	—	0.028
Mg	2.682	2.804	2.136	3.278	3.372	2.231	2.793	2.237	2.880	3.542	3.461	2.708	2.663
Ca	0.001	0.005	—	0.016	0.001	—	0.032	0.006	0.009	0.010	0.004	—	0.004
Na	0.018	0.012	0.018	0.033	0.024	—	0.007	0.032	0.030	0.045	0.018	0.015	—
K	1.670	1.723	1.694	1.790	1.826	1.891	1.738	1.595	1.819	1.790	1.765	1.741	1.799
Ni	—	0.005	—	0.005	0.009	0.006	—	0.005	0.009	—	0.007	0.008	—
X _{Fe}	0.477	0.440	0.579	0.394	0.339	0.556	0.476	0.583	0.456	0.351	0.366	0.487	0.499

* Total iron as FeO. X_{Fe}=Fe/(Fe+Mg).

Microprobe analyses of orthopyroxene, clinopyroxene, hornblende, biotite and plagioclase in these specimens were made using JEOL JXA-733 under such conditions as an acceleration voltage of 15 kV, beam currents of 0.012–0.015 μA and a beam diameter of 3 μ . Generally, several grains of each mineral species per specimen and two or more points per grain were analyzed. Except hornblende and plagioclase in some specimens, compositional zoning of each grain and compositional variations among one mineral species in each specimen are generally inconspicuous. Hornblende in Specimens B9* and B30 is weakly zoned in composition, *i.e.* its core is higher in Al_2O_3 content than its rim. Representative analyses of orthopyroxene, clinopyroxene, unzoned hornblende or the core of zoned hornblende and biotite are selected (Tables 3 to 6) and plotted on all the compositional diagrams presented below. Hornblende and plagioclase to be in contact with or proximate to each other are selected as their pairs shown in Fig. 7.

4. Mineral Compositions

The chemistry of orthopyroxene and clinopyroxene in all the pyroxene-bearing specimens can be represented by the following four main components: SiO_2 , FeO , MgO and CaO , because the other components are small in amount (Tables 3 and 4). The compositions of pyroxene are shown in Fig. 2. In Fig. 2, coexisting two-pyroxene

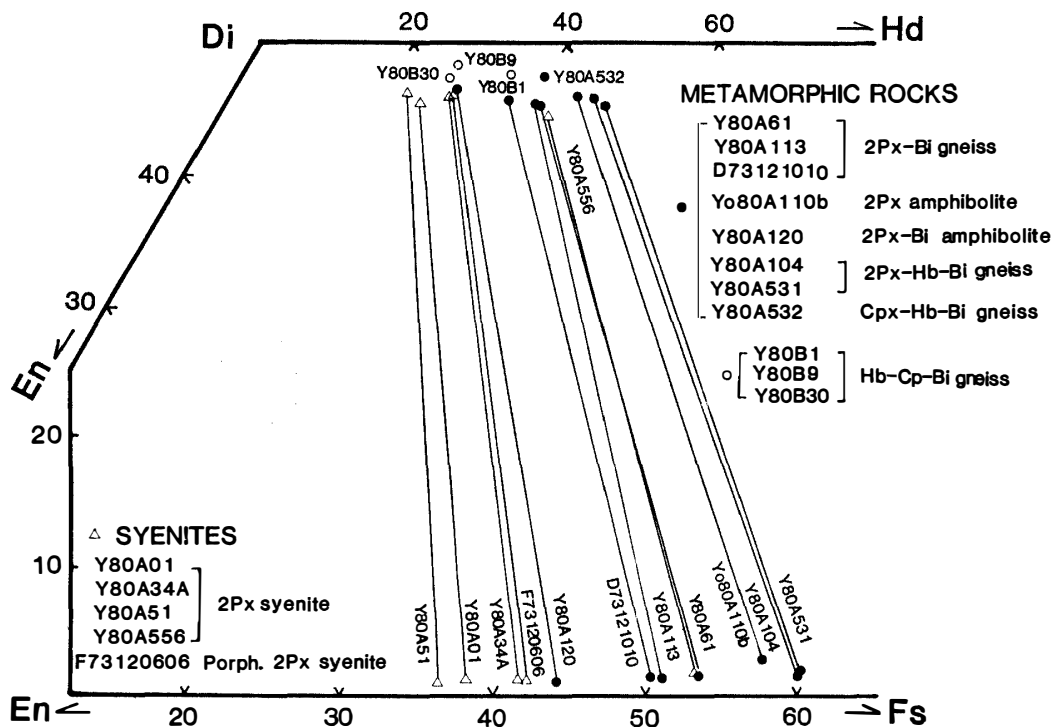


Fig. 2. $\text{CaSiO}_3\text{-MgSiO}_3\text{-FeSiO}_3$ diagram showing compositions of orthopyroxene and clinopyroxene, and phase relations of two-pyroxene pairs.

* In the text and figures, specimen numbers listed in Table 2 are expressed for simplification in such a way that Y80B9 is abbreviated to B9, D73121010 to D1010 and so on.

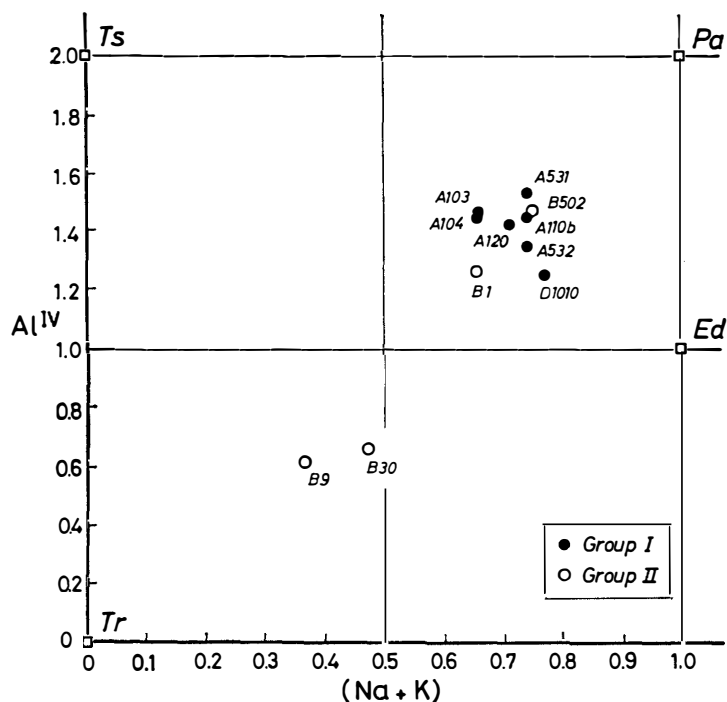


Fig. 3. $Al^{IV}-(Na+K)$ diagram for hornblende.

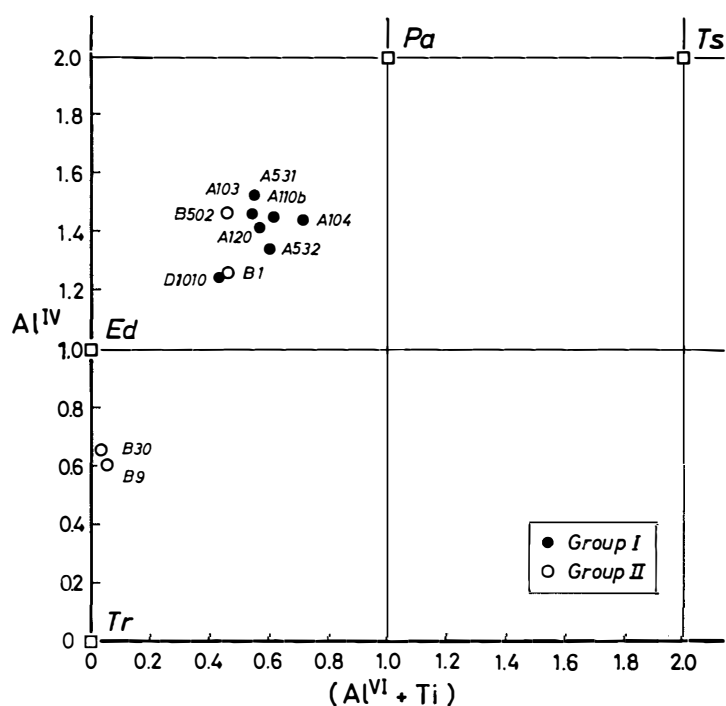


Fig. 4. $Al^{IV}-(Al^{VI}+Ti)$ diagram for hornblende.

pairs in the rocks of Group I are connected by tie lines. Clinopyroxene in all the specimens, B1, B9 and B30, of Group II and in Specimen A532 of Group I is a little poorer in $(Mg \cdot Fe)SiO_3$ component than that coexisting with orthopyroxene of Group I.

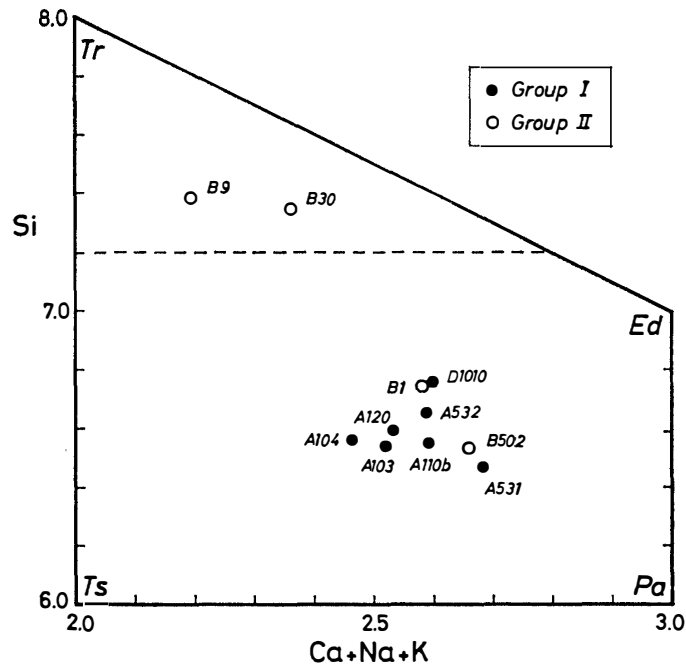


Fig. 5. $Si-(Ca+Na+K)$ diagram for hornblende.

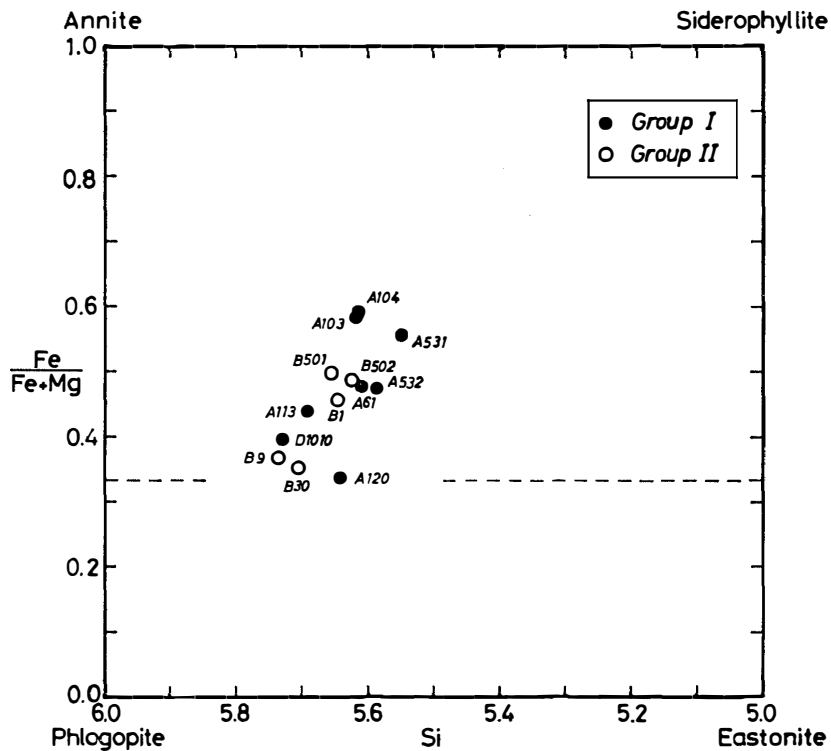


Fig. 6. $Fe/(Fe+Mg)$ -Si diagram for biotite.

The compositions of hornblende are plotted in Figs. 3, 4 and 5. These figures indicate that the compositions of hornblende of Group I are restricted to a small paragasitic field, whereas those of Group II range broadly from tremolitic to paragasitic ones.

Figure 6 shows the compositions of biotite. Biotite of Group I is similar in composition to that of Group II as far as plotted in Fig. 6, but the TiO_2 content of the former is generally somewhat higher than that of the latter (Table 6).

The anorthite content of plagioclase is given in Table 2. In some specimens, compositional heterogeneity is observed not only within one plagioclase grain but also among grains. In the former case, no regular compositional zoning from core to rim is found. The anorthite content of plagioclase is generally higher in the specimens of Group I than in those of Group II.

5. Mineral Parageneses

The basic to intermediate metamorphic rocks are composed mainly of such eleven components as SiO_2 , TiO_2 , Al_2O_3 , Fe_2O_3 , FeO , MnO , MgO , CaO , Na_2O , K_2O and H_2O . When minor Fe_2O_3 and MnO are neglected and H_2O is eliminated as a perfectly mobile component, mineral parageneses among mafic minerals and plagioclase in the rocks containing quartz and ilmenite or sphene may be approximately expressed in the system Al_2O_3 - FeO - MgO - CaO - Na_2O - K_2O . Biotite is also found as a chief K_2O -bearing phase in all the specimens. For consideration of phase relations among orthopyroxene,

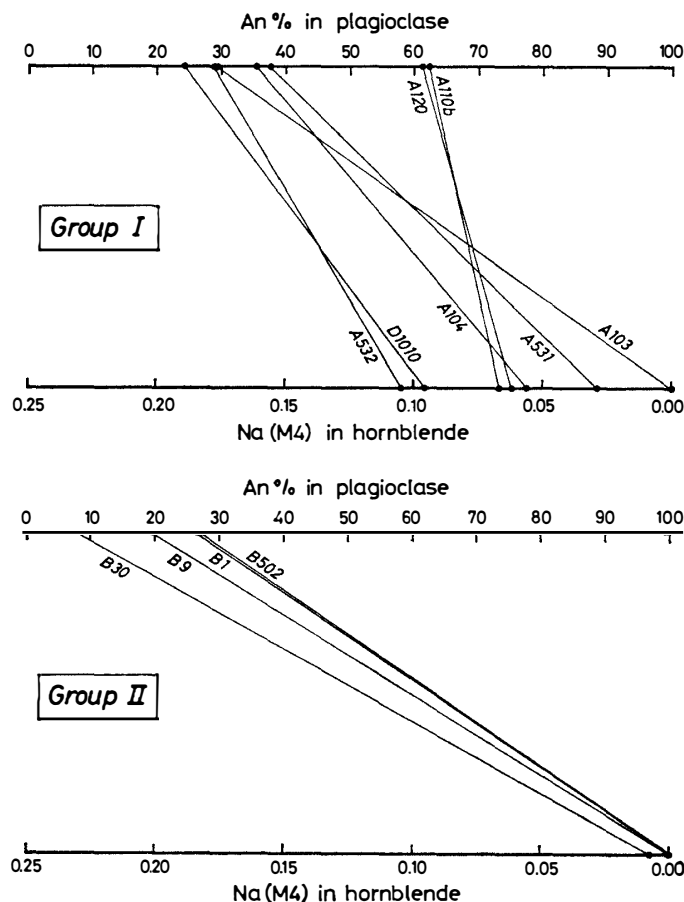


Fig. 7. $\text{Na}(\text{M}4)$ content of hornblende and anorthite content of coexisting plagioclase.

clinopyroxene, hornblende and plagioclase, the system may be more simplified to the Al_2O_3 -FeO-MgO-CaO- Na_2O one.

As obvious from the mineral compositions, Na_2O is exclusively concentrated in hornblende and plagioclase. When hornblende coexists with plagioclase, the Na_2O content of hornblende is controlled not only by metamorphic grade but also by the anorthite content of plagioclase (SPEAR, 1980). The distribution of Na and Ca between coexisting hornblende and plagioclase in the specimens examined here is shown in Fig. 7, where Na(M4) in hornblende was calculated by means of LEAKE (1978) assuming that total iron is ferrous. It is apparent from this figure that the Na content of hornblende depends on the anorthite content of coexisting plagioclase in each group, though the Na-Ca partition is not always consistent among all the specimens of Group I, and that $(Na/Ca)_{Hb}^{M4}/(Na/Ca)_{Pl}$ ratios of Group I are generally higher than those of Group II as exemplified by D1010 and A532 of Group I and B9, B1 and B502 of Group II all of which carry plagioclase of similar anorthite contents. These relations suggest that the hornblende-plagioclase assemblage of Group I is of higher grade than that of Group II (SPEAR, 1980).

Setting aside the Na-Ca distribution between hornblende and plagioclase, phase relations among orthopyroxene, clinopyroxene and hornblende in the rocks concerned may be considered in the Al_2O_3 -FeO-MgO-CaO system. These phase relations in

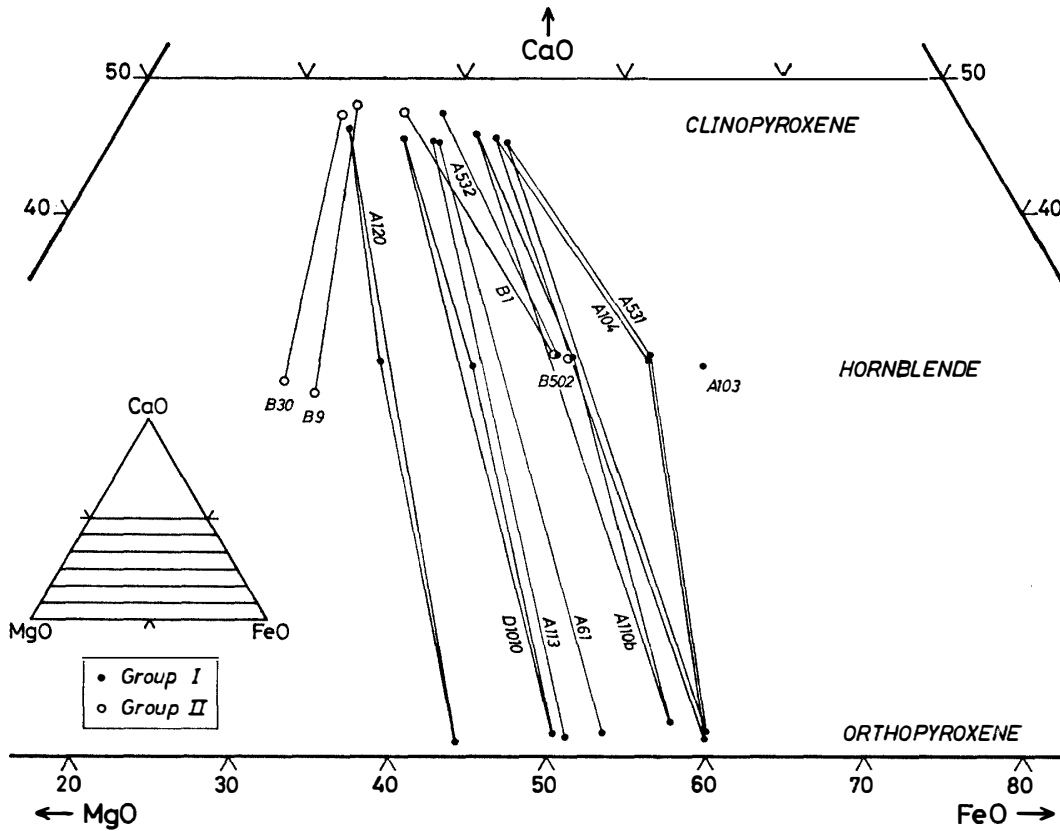


Fig. 8. CaO - MgO - FeO diagram showing phase relations of pyroxene and/or hornblende-bearing mineral assemblages. The assemblage in a quartz-free specimen A531 is also plotted for comparison.

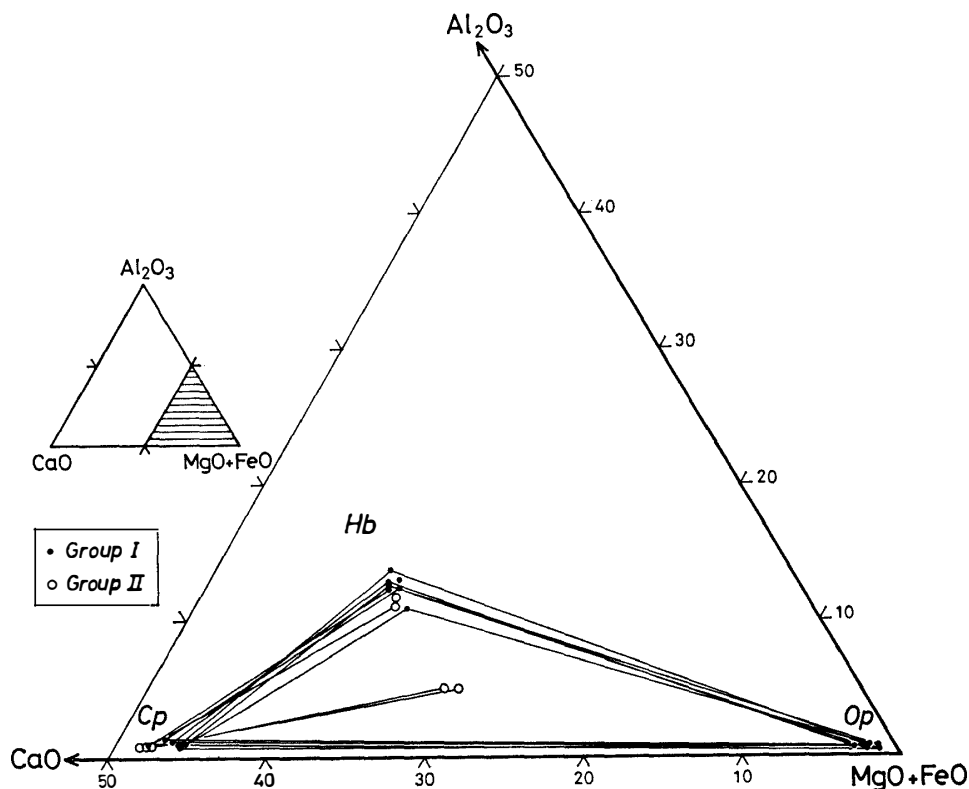
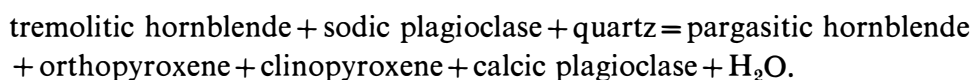


Fig. 9. Al_2O_3 -CaO-(MgO+FeO) diagram showing phase relations of hornblende-bearing mineral assemblages.

the Al_2O_3 -FeO-MgO-CaO tetrahedron are depicted using both the CaO-MgO-FeO diagram (Fig. 8) and Al_2O_3 -CaO-(MgO+FeO) diagram (Fig. 9). Figure 8 shows phase relations of the pyroxene- and/or hornblende-bearing assemblages of Groups I and II. Compatible relations are found among all of the three-phase (two-pyroxene-hornblende) triangles, two-pyroxene tie lines and a clinopyroxene-hornblende tie line of Group I, and between the clinopyroxene-hornblende tie lines of Group II except for the mineral pair in Specimen B1 which gives anomalous Mg-Fe distribution between the two minerals. The clinopyroxene-hornblende tie lines of Group I, however, are in incompatible relation to those of Group II. Figure 9 shows phase relations of the hornblende-bearing assemblages of Groups I and II. Figure 9 indicates that the compositions of hornblende of Group I are restricted to a small field relatively rich in Al_2O_3 , whereas the Al_2O_3 content of that of Group II is variable; that is, the clinopyroxene-hornblende tie lines of Group II are mostly included in the three-phase triangles of Group I. Thus, the mineral parageneses of Group I are incompatible with those of Group II in the Al_2O_3 -FeO-MgO-CaO tetrahedron.

It is suggested from the incompatible paragenetic relations in the system Al_2O_3 -FeO-MgO-CaO- Na_2O described above that the clinopyroxene-hornblende assemblage of Group II may not be stable under the granulite-facies conditions where the two-pyroxene-hornblende assemblage of Group I is stable. As shown in Figs. 8 and 9, the two-phase (clinopyroxene-hornblende) tie lines of Group II mostly lie within the

three-phase (two-pyroxene-hornblende) triangles of Group I; that is, the three-phase assemblage may be in isochemical relation to the two-phase assemblage in the Al_2O_3 -FeO-MgO-CaO system. The hornblende-plagioclase assemblage of Group II may also be in isochemical relation to that of Group I, because the tie lines of the former intersect those of the latter as shown in Fig. 7. Taking into account the compositional characters of hornblende (Figs. 3, 4, 5, 7 and 9), the different mineral parageneses between the two groups might be related by the following reaction:



Therefore, the hornblende-bearing assemblages of Group II are considered to represent those of the amphibolite facies.

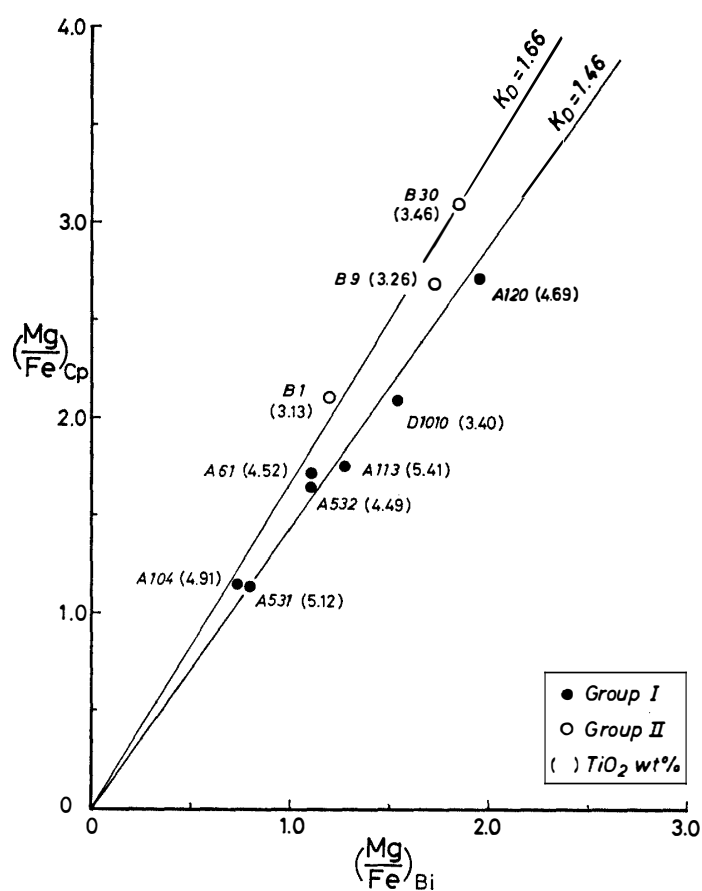


Fig. 10. Mg-Fe distribution between clinopyroxene and biotite.

Biotite is another Mg-Fe silicate common to all the specimens concerned. The Mg/Fe ratios of clinopyroxene and biotite are plotted in Fig. 10 to test equilibrium relations between the two minerals of each group. The Mg-Fe distribution between the two minerals of each group is considerably regular in spite of some variations of the TiO_2 content of biotite, and $K_{\text{D}_{\text{Mg-Fe}}^{\text{Cp-Bi}}}$ of Group I is lower than that of Group II. Such relations suggest that biotite in each specimen coexists in equilibrium with clino-

pyroxene, and that the difference in $K_D^{Cp-Bi}_{Mg-Fe}$ between Groups I and II reflects the different metamorphic conditions as mentioned above.

6. Geological Relations of the Granulite-facies and Amphibolite-facies Rocks

We have found no contact of the granulite-facies rocks with the amphibolite-facies rocks in the Yamato Mountains (SHIRAIISHI *et al.*, 1982b). However, it is possible to infer indirectly the mutual relations between the two groups from geological and petrological relations of the syenitic rocks to each group of the metamorphic rocks.

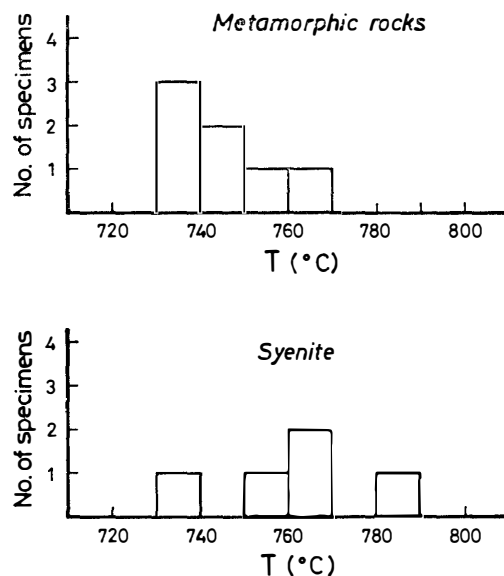


Fig. 11. Two-pyroxene solvus temperatures, after WOOD and BANNO (1973) and WOOD (1975), for metamorphic rocks and associated syenitic rocks.

Orthopyroxene-clinopyroxene-bearing assemblages are widely recognized in metamorphic rocks in Massif D and those intimately associated with the syenitic rocks in Massifs A and G, and in paleosomes of the migmatitic gneiss in Massifs D and F (Fig. 1). Two-pyroxene phase relations and two-pyroxene geothermometry after WOOD and BANNO (1973) for the metamorphic rocks are shown in Figs. 2 and 11, respectively, together with those for the associated syenitic rocks. In Fig. 11, temperatures after subtracting 60°C from WOOD and BANNO's temperatures are given after WOOD (1975). The tie-line relations in Fig. 2 are compatible with each other not only among the metamorphic rocks and among the syenitic rocks but also between both. Temperatures obtained from the metamorphic rocks fall consistently in a small range of 730–770°C, and those from the syenitic rocks, 730–790°C, are very close to the former ones (Fig. 11). The two-pyroxene-bearing gneiss and amphibolite of Group I in Massifs A and G are enclosed as small masses or inclusions in the syenitic rocks but show no textural sign of thermal recrystallization. These geological and petrological characters suggest that the two-pyroxene-bearing metamorphic rocks were formed

under uniform P-T conditions of the granulite facies in spite of their various modes of occurrence, and that the syenitic rocks were emplaced during the granulite-facies metamorphism which produced the metamorphic rocks of Group I.

On the other hand, the granitic gneiss and associated metamorphic rocks of the amphibolite facies occur as large masses in Massifs B, C and D, and are in contact with the syenitic rocks (Fig. 1). The contact relations between these metamorphic rocks and the syenitic rocks, however, are of tectonic: being a thrust fault in Massif C and an intensely deformed narrow zone composed mainly of gneissose granite in Massif D (SHIRAISHI *et al.*, 1982b).

Therefore, the granulite-facies rocks and the associated syenitic rocks are considered to form a geological unit which differs from the other unit of the amphibolite-facies rocks. It is probable that each unit was laid on different crustal levels or occupied different grade portions of a metamorphic sequence prior to the tectonic movement; however, the tectonic and metamorphic history of each unit has been left for future studies.

Acknowledgments

We are indebted to Prof. T. NUREKI of Okayama University for his critical review of an earlier draft of the manuscript. The field work in 1980 was made with the cooperation of Dr. Y. OHTA of Norsk Polarinstitut, to whom we would like to extend our thanks.

References

- KIZAKI, K. (1965): Geology and petrography of the Yamato Sanmyaku, East Antarctica. *JARE Sci. Rep., Ser. C (Geol.)*, **3**, 27p.
- LEAKE, B. E. (1978): Nomenclature of amphiboles. *Mineral. Mag.*, **42**, 533–563.
- OHTA, Y. and KIZAKI, K. (1966): Petrographic studies of potash feldspar from the Yamato Sanmyaku, East Antarctica. *JARE Sci. Rep., Ser. C (Geol.)*, **5**, 40p.
- SHIRAISHI, K. (1977): Geology and petrography of the northern Yamato Mountains, East Antarctica. *Mem. Natl Inst. Polar Res., Ser. C (Earth Sci.)*, **12**, 33p.
- SHIRAISHI, K., KIZAKI, K., YOSHIDA, M. and MATSUMOTO, Y. (1978): Mt. Fukushima, northern Yamato Mountains. *Antarct. Geol. Map Ser., Sheet 27(1)* (with explanatory text 7p., 2 pl.). Tokyo, Natl Inst. Polar Res.
- SHIRAISHI, K., ASAMI, M. and OHTA, Y. (1982a): Plutonic and metamorphic rocks of Massif-A in the Yamato Mountains, East Antarctica. *Mem. Natl Inst. Polar Res., Spec. Issue*, **21**, 21–31.
- SHIRAISHI, K., ASAMI, M. and OHTA, Y. (1982b): Geology and petrology of the Yamato Mountains. submitted to *Antarctic Earth Science; Proc. 4th Symp.*, Adelaide, 1982.
- SHIRAISHI, K., ASAMI, M. and KANAYA, H. (1983): Petrochemical character of the syenitic rocks from the Yamato Mountains, East Antarctica. *Mem. Natl Inst. Polar Res., Spec. Issue*, **28**, 183–197.
- SPEAR, F. S. (1980): $\text{NaSi} \rightleftharpoons \text{CaAl}$ exchange equilibrium between plagioclase and amphibole. *Contrib. Mineral. Petrol.*, **72**, 33–41.
- WOOD, B. J. (1975): The influence of pressure, temperature and bulk composition on the appearance of garnet in orthogneisses; An example from South Harris, Scotland. *Earth Planet. Sci. Lett.*, **26**, 299–311.
- WOOD, B. J. and BANNO, S. (1973): Garnet-orthopyroxene and orthopyroxene-clinopyroxene relationships in simple and complex systems. *Contrib. Mineral. Petrol.*, **42**, 109–124.

- YANAI, K., NISHIDA, T., KOJIMA, H., SHIRAISHI, K., ASAMI, M., OHTA, Y., KIZAKI, K. and MATSUMOTO, Y. (1982): The central Yamato Mountains, Massif B and Massif C, Antarctica. *Antarct. Geol. Map Ser.*, Sheet **28** (with explanatory text 10p., 6pl.). Tokyo, Natl Inst. Polar Res.
- YOSHIDA, M. and ANDO, H. (1971): Geological surveys in the vicinity of Lützow-Holm Bay and the Yamato Mountains, East Antarctica. *Nankyoku Shiryo* (*Antarct. Rec.*), **39**, 46-54.

(Received April 30, 1983; Revised manuscript received June 20, 1983)